energies

MDPI

Article

Thermophysical Properties of 1-Butanol at High Pressures †

Marzena Dzida

Institute of Chemistry, University of Silesia in Katowice, Szkolna 9, 40-006 Katowice, Poland; marzena.dzida@us.edu.pl; Tel.: +48-323591643

† In memoriam Michał Zorębski, M.Sc. (1960–2020).

Received: 30 August 2020; Accepted: 21 September 2020; Published: 25 September 2020

Abstract: 1-Butanol can be considered as a good fuel additive, which can be used at high pressures. Therefore, the knowledge of high-pressure thermophysical properties is crucial for this application. In this paper, new experimental data on the speed of sound in 1-butanol in the temperature range from 293 to 318 K and at pressures up to 101 MPa are reported. The speed of sound at a frequency of 2 MHz was measured at atmospheric and high pressures using two measuring sets operating on the principle of the pulse–echo–overlap method. The measurement uncertainties were estimated to be better than ±0.5 $m \cdot s^{-1}$ and ± 1 $m \cdot s^{-1}$ at atmospheric and high pressures, respectively. Additionally, the density was measured under atmospheric pressure in the temperature range from 293 to 318 K using a vibrating tube densimeter Anton Paar DMA 5000. Using the experimental results, the density and isobaric and isochoric heat capacities, isentropic and isothermal compressibilities, isobaric thermal expansion, and internal pressure were calculated at temperatures from 293 to 318 K and at pressures up to 100 MPa.

Keywords: 1-butanol; speed of sound; density; isobaric heat capacity; high pressure

1. Introduction

1-Butanol is an important chemical platform used as feedstock in the plastic industry, plasticizers, paints, binders and food extractant. However, much attention has been paid to the use of 1-butanol as a fuel. 1-Butanol can be used as an additive for gasoline, diesel, and kerosene or as an alternative fuel [1–4]. Studies show that the use of 1-butanol for this purpose is much more advantageous than the use of ethanol. 1-Butanol has higher energy density, lower than ethanol vapor pressure and improved miscibility with gasoline, lower solubility in water and it is less corrosive than ethanol [2,5,6]. Currently, 1-butanol is produced almost entirely from petroleum and the global demand for 1-butanol is about 2.8 metric tons per year [1]. The International Energy Agency forecasts that the demand for biofuels will be 690 million tons per year in 2050 [1]. The strong renewed interest in 1-butanol as a sustainable vehicle fuel has led to the development of improved biobutanol production processes including both biotechnological production processes as well as separation techniques [1,7–11]. Various species of the *Clostridium* bacteria such as *C. acetobutylicum*, *C. beijerinckii*, *C. saccharoperbutylacetonicum* and *C. saccharobutylicum* are mainly used for 1-butanol production [7]. However, *Clostridium* can be genetically modified in order to increase its ability to produce 1-butanol, and others have extracted enzymes from bacteria and incorporated them into other microbes such as yeast in order to turn them into 1-butanol production. Yeast (for example, *Sacharomyces cerevisiae* [8]) and *Escherichia coli*, one of the major bacteria in the human gut, are believed to be easily grown on an industrial scale [7]. The produced biobutanol can be separated by several methods including adsorption, gas stripping pervaporation, and liquid–liquid extraction using, for example, ionic liquids [6,8,11]. The next stage is the test of the properties of biobutanol in terms of its use in engines. In the injection systems used in automotive engines, the pressure can reach 250 MPa and the fuel injection takes place under

adiabatic conditions [12]. Therefore, the petrochemical industry is interested in the thermodynamic and acoustic properties of fuel biocomponents under high pressures. Although 1-butanol has many important applications, especially as a fuel additive or intrinsic biofuel, the high-pressure speed of sound in this alcohol is still incomplete. There are only two available datasets. The speed of sound in primary alcohols under high pressures has been measured by Sysoev and Otpuschennikov and published in Nauchnye Trudy (Kurskiœi Gosudarstvennyœi Pedagogicheskiœi Institute) [13]. However, these data are not available. Khasanshin [14] published a correlation equation for the speed of sound in 1-alkanols with the carbon atoms in the chain ranging from 4 to 12 at pressures from (0.1 to 100) MPa and at six temperatures from (303.15 to 453.15) K determined at 20 K steps using the above-mentioned experimental data [13]. Plantier et al. [15] measured the speed of sound in 1-butanol at temperatures from (303.15 to 373.15) K at pressures up to 50 MPa. More literature data are available for the high-pressure density of 1-butanol. Recently, Safarov et al. [16] reported the experimental density of 1-butanol in the temperature range from (263.15 to 468.15) K and at pressures up to 140 MPa and they provided a careful literature search on experimental high-pressure density reported up to now. They also calculated the high-pressure speed of sound in 1-butanol using pressure dependence of density. Additionally, Dávila et al. [17] measured the density of 1-butanol over the temperature range from (278.15 to 358.15) K and at pressures up to 60 MPa. Khasanshin [18] published a correlation equation between the density and the number of carbon atoms ranging from 4 to 10 at pressures up to 50 MPa at 293.15 K and at 298.15 K. Cibulka and Zíková [19] also reported correlation equations of the Tait type based on the $p\rho T$ data published by different authors before 1993.

This work is the completion of systematic research on the high-pressure thermodynamic and acoustic properties of 1-akanols [20,21]. In this paper, new experimental speed of sound data are reported for 1-butanol in the temperature range from (293 to 318) K and at pressures up to 101 MPa. To the best of my knowledge, measurement of the speed of sound has never been conducted in this temperature and pressure range. Additionally, the density data under atmospheric pressure in the temperature range from (293 to 318) K are presented. Using the experimental results of speed of sound as a function of temperature and pressure, the temperature dependence of density under atmospheric pressure and the temperature dependence of isobaric heat capacity under atmospheric pressure reported by Zábranský et al. [22], the thermodynamic characteristics of compressed 1-butanol were obtained for temperatures from (293 to 318) K and for pressures from (0.1 to 100) MPa. The temperature and pressure dependence of density $\rho(T, p)$, the temperature and pressure dependence of isobaric heat capacity $C_p(T, p)$, and related quantities such as isentropic compressibility, κ_S, isobaric thermal expansion, α_p, isothermal compressibility, κ_T, isochoric heat capacity, C_V, and internal pressure, p_{int}, were calculated. The method proposed by Davis and Gordon [23] with a numerical procedure described by Sun et al. [24] was applied for calculations. This study is aimed first to compare pressure dependence of density, isentropic compressibility and isobaric thermal expansion of 1-butanol with those of biocomponents or components of fuels such as ethanol, heptane, dodecane as well as biodiesel (fatty acid methyl esters of rapeseed oil, FAME) and low sulphur diesel oil (ekodiesel ultra), in the context of the use of 1-butanol as a fuel additive or alternative fuel. To the best of my knowledge, such analyses have never been performed to date. The second aim is to find whether the changes in properties of 1-butanol, caused by temperature and pressure, are reflected in the internal pressure.

2. Experimental Section

2.1. Chemical

The 1-butanol (0.998 mass fraction purity of C_4H_9OH) was purchased from Aldrich. Alcohol was dried over molecular sieves 0.3 nm. The mass fraction of water, determined by the Karl Fischer method, was less than $1 \cdot 10^{-4}$. The purity of 1-butanol was tested by comparison of the measured speed of sound and density at 0.1 MPa with literature data (Table 1). Additionally, the comparison of the results obtained of this work (y_{exp}) and literature values (y_{lit}) were presented as the relative

deviation $RD/\% = 100 \cdot (y_{exp} - y_{lit})/y_{exp}$. The relative deviations between the speed of sound at ambient pressure obtained of this work and literature values are in the range from −0.11% [15] to 0.013% [25] (Figure 1). The relative deviations between density at ambient pressure obtained of this work and literature values are in the range from −0.016% [16] to 0.018% [26] (Figure 2).

Table 1. Comparison of the speed of sound, u, and density, ρ, at atmospheric pressure obtained in this work with those reported in the literature.

	***T* (K)**	**This Work**	**Literature**
u (m·s^{-1}) *	293.15	1256.33	1256.25 [25], 1256.8 [26], 1257.5 [27]
	298.15	1239.29	1239.2 [28], 1239.22 [25], 1239.29 [29] 1239.3 [27], 1239.39 [30,31], 1239.8 [26]
	303.15	1222.36	1222.25 [25],1222.36 [14], 1222.4 [27] 1222.9 [26], 1223.6 [15]
	308.15	1205.54	1205.53 [25], 1205.79 [32], 1206.2 [26]
	313.15	1188.81	1188.65 [25], 1189.6 [26], 1190.1 [15]
	318.15	1172.19	1173.0 [26]
ρ (kg·m^{-3}) **	293.15	809.58	809.5 [26], 809.60 [27], 809.64 [16]
	298.15	805.79	805.7 [26], 805.770 [30], 805.77 [16] 805.78 [27]
	303.15	801.95	801.9 [26], 801.928 [30], 801.94 [27]
	308.15	798.10	798.0 [26], 798.054 [30]
	313.15	794.22	794.1 [26], 794.146 [30], 794.35 [16]
	318.15	790.24	790.1 [26], 790.196 [30]

* calculated from Equation (1); ** experimental data.

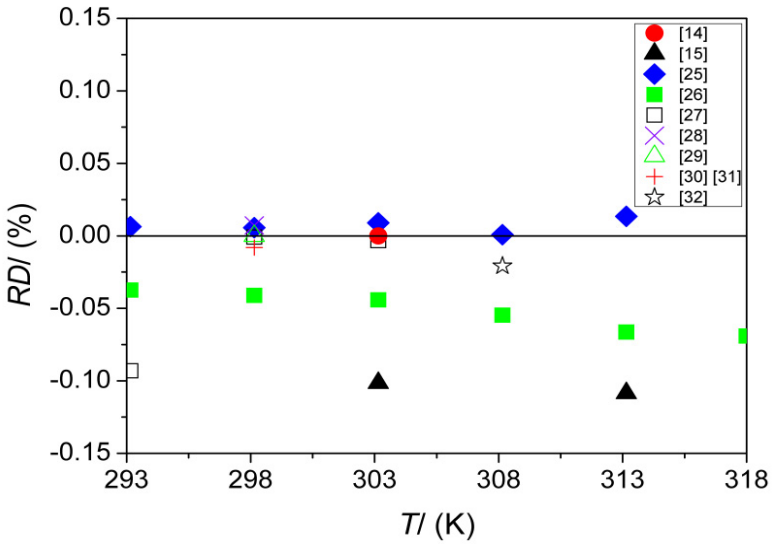

Figure 1. Comparison of the speed of sound in 1-butanol as a function of temperature under atmospheric pressure obtained in this work ($u_{this\ work}$) with the literature values (u_{lit}) [14,15,25–32] presented as relative deviations *RD*s ($RD/\% = 100 \cdot (u_{this\ work} - u_{lit})/u_{this\ work}$).

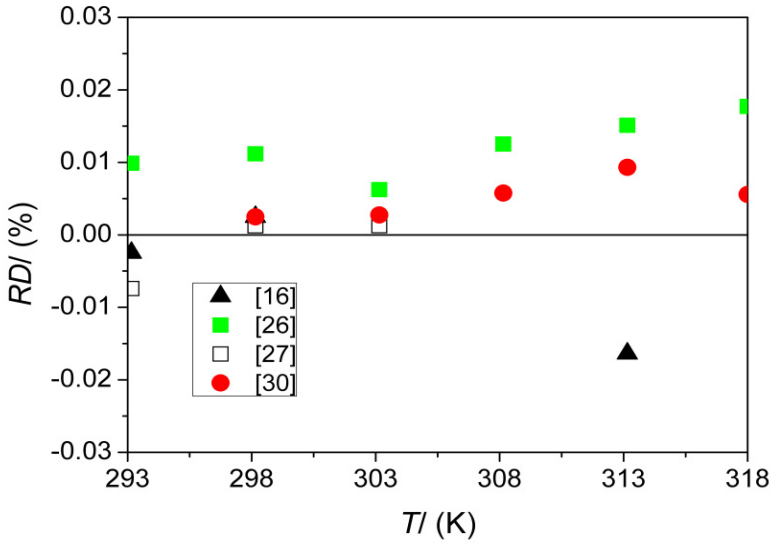

Figure 2. Comparison of the density of 1-butanol as a function of temperature under atmospheric pressure obtained in this work ($\rho_{\text{this work}}$) with the literature values (ρ_{lit}) [16,26,27,30] presented as relative deviations *RD*s ($RD/\% = 100 \cdot (\rho_{\text{this work}} - \rho_{\text{lit}})/\rho_{\text{this work}}$).

2.2. Speed of Sound Measurements

The speed of sound measurements were conducted at ambient and high pressures using two measuring sets operate based on the pulse–echo–overlap method with measuring vessels of the same acoustic path and constructed by a single transmitting–receiving ceramic transducer of 2 MHz and an acoustic mirror. The pressure was measured using a strain gauge measuring system (Hottinger Baldwin System P3MD) with accuracy better than 0.15%. During measurements, the pressure stability was ±0.03 MPa. The temperature was measured by an Ertco Hart 850 platinum resistance thermometer (NIST certified) with an uncertainty of ±0.05 K and resolution of 0.001 K. During measurements, the stability of temperature was ±0.005 K at ambient pressure and ±0.01 K at high pressures. The uncertainties of the speed of sound measurements under ambient and high pressures were estimated to be better than ±0.5 $m \cdot s^{-1}$ and ±1 $m \cdot s^{-1}$, respectively. The details concerning the construction of a high-pressure device as well as the method of the speed of sound measurements and calibration can be found in the previous paper [33].

2.3. Density Measurements

The density was measured at atmospheric pressure using a vibrating tube densimeter Anton Paar DMA 5000. The calibration was conducted using the extended procedure with dry air and re-distilled water. The uncertainty of the density measurements was estimated to be ±0.05 $kg \cdot m^{-3}$.

3. Results and Discussion

The speed of sound in 1-butanol was measured from (293 to 318) K in about 5 K steps and under the pressures up to 101.34 MPa. The experimental values are listed in Table 2. The relative deviations *RDs* between the high-pressure speed of sound obtained of this work and literature values are in the range from 0.12% [15] to −3.3% [16] (see Figure 3). Additionally, the absolute average relative deviations (*AARDs*) between results obtained in this work (y_{exp}) and the literature values (y_{lit}) were calculated as $AARD = (100/N) \sum_{i=1}^{n} \left| (y_{\text{exp},\,i} - y_{\text{lit},\,i}) / y_{\text{exp},\,i} \right|$ (where N is the number of data points). The *AARDs* equal 0.03% [14], 0.08% [15], and 1.1% [16].

Table 2. The experimental speed of sound, u, in 1-butanol measured at pressures up to 101.34 MPa within the temperature range from (293 to 318) K.

T (K)	p (MPa)	u (m·s^{-1})	T (K)	p (MPa)	u (m·s^{-1})	T (K)	p (MPa)	u (m·s^{-1})
292.65	0.1	1258.06	303.16	0.1	1222.26	313.16	0.1	1188.85
292.86	15.2	1336.38	302.98	15.21	1304.62	313.10	15.21	1274.40
292.85	30.39	1406.63	302.97	30.39	1376.93	313.13	30.39	1348.79
292.85	45.59	1470.61	303.00	45.59	1442.45	313.12	45.59	1416.05
292.85	60.80	1529.80	302.98	60.80	1502.93	313.11	60.79	1477.91
292.87	76.00	1583.46	303.05	76.00	1557.55	313.11	76.01	1533.90
292.87	91.19	1633.68	303.01	91.19	1608.67	313.03	91.19	1585.65
292.83	101.32	1665.21	302.98	101.33	1640.91	312.99	101.33	1618.69
298.16	0.1	1239.24	308.16	0.1	1205.55	318.60	0.1	1170.66
298.00	15.20	1319.99	308.00	15.2	1289.43	318.52	15.18	1257.86
298.00	30.40	1391.35	308.01	30.39	1362.92	318.52	30.39	1333.80
297.99	45.59	1456.21	308.00	45.59	1429.35	318.47	45.60	1402.24
297.99	60.79	1516.04	308.03	60.79	1490.34	318.46	60.80	1464.54
298.00	75.99	1570.22	307.99	76.00	1545.86	318.45	76.01	1521.23
298.00	91.19	1620.86	307.99	91.19	1596.96	318.45	91.19	1573.46
297.99	101.34	1652.77	308.02	101.33	1629.34	318.46	101.34	1606.71

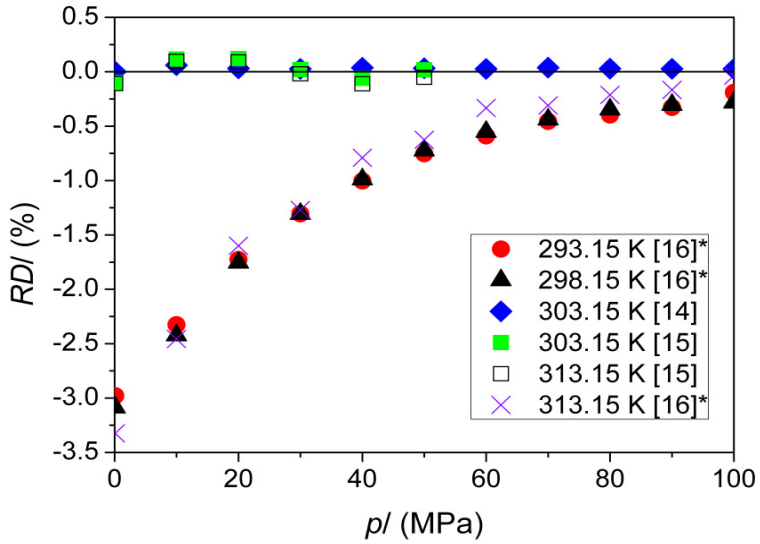

Figure 3. Comparison of the speed of sound in 1-butanol as a function of pressure obtained in this work ($u_{\text{this work}}$) with the literature values (u_{lit}) [14–16] presented as relative deviations RDs (RD/% = 100·($u_{\text{this work}}$−u_{lit})/$u_{\text{this work}}$); * calculated from the $p\rho T$ data [16].

The density of the alcohol under test was measured under atmospheric pressure within the temperature range from (293.15 to 318.15) K. The experimental values are collected in Table 1.

The dependence of the speed of sound and density on the temperature at atmospheric pressure was approximated by the second-order polynomial:

$$y = \sum_{j=0}^{2} b_j T^j, \tag{1}$$

where y is the speed of sound, u_0, or density, ρ, at atmospheric pressure p_0, bj are the polynomial coefficients ($b_j = c_j$ for the speed of sound, and $b_j = \rho_j$ for the density) calculated by the least-squares method. The backward stepwise rejection procedure was used to reduce the number of non-zero coefficients. The coefficients and standard deviations from the regression lines are provided in Table 3.

Table 3. Coefficients of polynomial (1) for the speed of sound and density.

c_0 (m·s^{-1})	c_1 (m·s^{-1}·K^{-1})	c_2·10^3 (m· s^{-1}·K^{-2})	δu_0 [a] (m·s^{-1})
2436.59	−4.63487	2.07654	0.07
ρ_0 (kg·m^{-3})	ρ_1 (kg·m^{-3}·K^{-1})	ρ_2·10^4 (kg·m^{-3}·K^{-2})	$\delta\rho$ [a] (kg·m^{-3})
964.750	−0.304950	−7.65424	0.01

[a] mean deviation from the regression line.

The speed of sound dependence on pressure and temperature was approximated using the equation proposed by Sun et al. [24]:

$$p - p_0 = \sum_{i=1}^{3} \sum_{j=0}^{2} a_{ij} (u - u_0)^i T^j, \tag{2}$$

where a_{ij} are the polynomial coefficients calculated by the least-squares method, u is the speed of sound at $p > 0.1$ MPa, u_0 is the speed of sound at ambient pressure, calculated from Equation (1). The coefficients a_{ij} and the mean deviation from the regression line are provided in Table 4. The stepwise rejection procedure was used to reduce the number of non-zero coefficients.

Table 4. Coefficients of Equation (2).

	a_{1j}	a_{2j}	a_{3j}	δu [a]
	(K^{-j}·MPa·s·m^{-1})	(K^{-j}·MPa·s^2·m^{-2})	(K^{-j}·MPa·s^3·m^{-3})	(m·s^{-1})
j				
0	0.282824	1.38485·10^{-4}	1.37252·10^{-7}	0.29
1	-	-	-	
2	−1.20119·10^{-6}	-	7.92802·10^{-13}	

[a] mean deviation from the regression line.

The density and isobaric heat capacity of 1-butanol were determined for temperatures from (293 to 318) K and for pressures up to 100 MPa using the acoustic method. In the calculations, the experimental speed of sound data as a function of temperature and pressure were used, together with the temperature dependence of density and isobaric heat capacity at atmospheric pressure. The temperature dependence of the isobaric heat capacity reported by Zábranský et al. [22] was used.

The applied acoustic method is based mainly on the thermodynamic relationship between isothermal compressibility κ_T and isentropic compressibility κ_S:

$$\kappa_T = \kappa_S + \frac{\alpha_p^2 \cdot T}{\rho \cdot c_p}, \tag{3}$$

where c_p is the specific isobaric heat capacity and α_p is the isobaric thermal expansion defined as:

$$\alpha_p \equiv -\rho^{-1} \cdot (\partial\rho/\partial T)_p. \tag{4}$$

The substitution the Laplace formula:

$$\kappa_S = \frac{1}{\rho u^2}, \tag{5}$$

and definition of isothermal compressibility:

$$\kappa_T \equiv \rho^{-1} \cdot (\partial\rho/\partial p)_T, \tag{6}$$

into Equation (3) leads to the following relationship:

$$\left(\frac{\partial \rho}{\partial p}\right)_T = \frac{1}{u^2} + \frac{T\alpha_p^2}{c_p}. \tag{7}$$

The change of density, $\Delta\rho$, caused by the change of pressure from p_1 to p_2 at constant temperature T can be approximated sufficiently accurate as follows:

$$\Delta\rho = \int_{p_1}^{p_2}\left(\frac{1}{u^2} + \frac{\alpha_p^2 T}{c_p}\right)dp \approx \int_{p_1}^{p_2}\frac{1}{u^2}dp + \frac{\alpha_p^2 T}{c_p}\Delta p, \tag{8}$$

provided that $\Delta p = p_2 - p_1$ is small. The initial values of $u(T, p_0 = 0.101325\ \text{MPa})$, $\rho(T, p_0 = 0.101325\ \text{MPa})$, and $c_p(T, p_0 = 0.101325\ \text{MPa})$ were used in the Equation (8). The specific isobaric heat capacity at p_2 is acquired by:

$$c_p(p_2) \approx c_p(p_1) - (T/\rho)\left\{\alpha_p^2 + (\partial\alpha_p/\partial T)_p\right\}\Delta p, \tag{9}$$

where $c_p(p_1)$ is the specific isobaric heat capacity at p_1. The uncertainties of the density and specific isobaric heat capacity estimated using the perturbation method are ±0.02% and ±0.3%, respectively. The expanded uncertainties were estimated to be better than $U(\rho) = 5{\cdot}10^{-4}{\cdot}\rho$ kg·m^{-3} and $U(C_p)=1{\cdot}10^{-2}{\cdot}C_p$ J·mol^{-1}·K^{-1} for density and molar isobaric heat capacity, respectively. The density and molar isobaric heat capacity at high pressures are collected in Tables 5 and 6, respectively.

Table 5. The density, ρ, of 1-butanol at pressures up to 100 MPa and within the temperature range from (293 to 318) K.

***p* (MPa)**	**ρ (kg·m^{-3})**					
	***T* (K)**					
	293.15	298.15	303.15	308.15	313.15	318.15
0.1 *	809.58	805.79	801.96	798.10	794.20	790.26
10	816.60	812.99	809.36	805.69	801.98	798.24
20	823.12	819.67	816.19	812.68	809.14	805.57
30	829.18	825.86	822.52	819.15	815.75	812.32
40	834.86	831.66	828.43	825.18	821.90	818.59
50	840.20	837.11	833.99	830.84	827.67	824.47
60	845.27	842.27	839.24	836.19	833.11	830.00
70	850.08	847.17	844.23	841.26	838.27	835.25
80	854.67	851.84	848.98	846.09	843.17	840.23
90	859.06	856.30	853.51	850.70	847.86	844.99
100	863.27	860.58	857.86	855.12	852.34	849.54

* calculated from Equation (1).

Table 6. The isobaric molar heat capacity, C_p, of 1-butanol at pressures up to 100 MPa and within the temperature range from (293 to 318) K.

***p* (MPa)**	**C_p (J·mol^{-1}·K^{-1})**					
	***T* (K)**					
	293.15	298.15	303.15	308.15	313.15	318.15
0.1 *	173.70	177.17	180.82	184.62	188.57	192.62
10	172.8	176.2	179.9	183.6	187.5	191.5
20	172.0	175.4	179.0	182.7	186.6	190.6
30	171.3	174.7	178.2	181.9	185.8	189.7
40	170.6	174.0	177.5	181.2	185.0	188.9

Table 6. *Cont.*

p (MPa)	C_p (J·mol^{-1}·K^{-1})					
	T (K)					
50	170.0	173.4	176.9	180.5	184.3	188.2
60	169.4	172.7	176.2	179.8	183.6	187.5
70	168.8	172.2	175.6	179.2	183.0	186.8
80	168.3	171.6	175.0	178.6	182.3	186.2
90	167.8	171.1	174.5	178.0	181.7	185.6
100	167.2	170.5	173.9	177.5	181.2	185.0

* values from ref. [22].

The density of 1-butanol obtained in this work was compared with the experimental data reported by 1993, correlated by Cibulka and Ziková [19]. The *RD*s are in the range from 0.02 to 0.09% (see Figure 4). The *AARD* was found to be 0.04%. Particularly, the attention has been paid to excellent agreement between the raw density reported by Zúñiga–Moreno et al. [34] and density obtained in this work as follows: 801.97 kg·m^{-3} at 313.10 K, 9.996 MPa [34] and 801.98 kg·m^{-3} at 313.15 K, 10 MPa as well as 809.14 kg·m^{-3} at 313.10 K, 20.015 MPa [34] and 809.14 kg·m^{-3} at 313.15 K, 20 MPa. A good agreement was found also for data reported by Dávila et al. [17]. The *RD*s are in the range from −0.13% to −0.004% (see Figure 4), the *AARD* is 0.07%. The density obtained in this work is also in very good agreement with those reported by Safarov et al. [16], the *RD*s are in the range from −0.04 to 0.08% (see Figure 4) and *AARD* equals 0.04%. Thus, again the density calculated by the indirect, acoustic method is in an excellent agreement with density measured by high-pressure vibrating tube densimeter. On the other hand, the speed of sound calculated from experimental $\rho(p,T)$ data is in worse agreement with experimental ones (see Figure 3). This was discussed in detail in the previous work [35]. Using both the acoustic method and densimetric one, the $C_p(p,T)$ data can be obtained by the same relationship (Equation (6)). The agreement between the $C_p(p,T)$ data obtained by the acoustic method (this work) and densimetric one (reported by Safarov et al. [16]) is excellent, the *RD*s are in the range from −0.67 to 0.17% and *AARD* is 0.22% (see Figure 5).

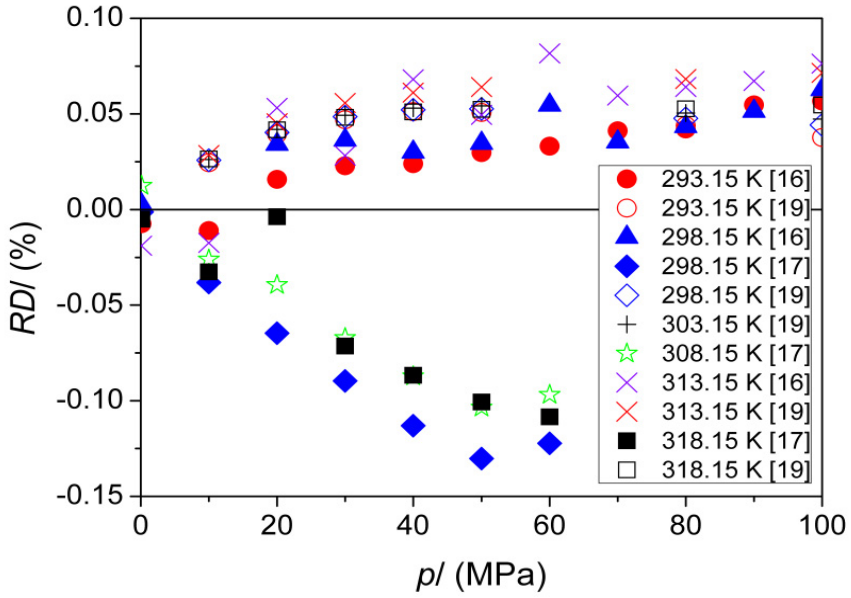

Figure 4. Comparison of the density of 1-butanol as a function of pressure obtained in this work ($\rho_{\text{this work}}$) with the literature values (ρ_{lit}) [16,17,19] presented as relative deviations *RD*s ($RD/\% = 100\cdot(\rho_{\text{this work}}-\rho_{\text{lit}})/\rho_{\text{this work}}$).

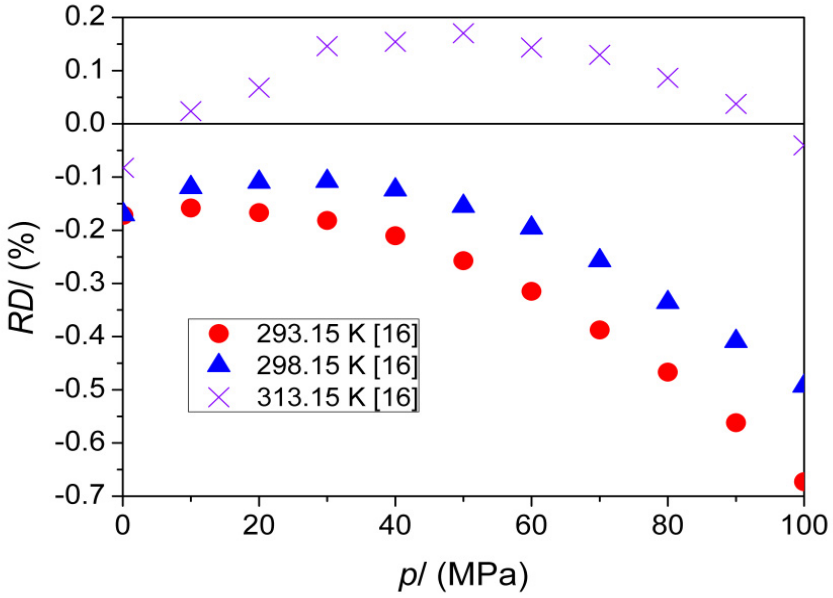

Figure 5. Comparison of the isobaric heat capacity of 1-butanol as a function of pressure obtained in this work ($C_{p,\text{this work}}$) with the literature values ($C_{p,\text{lit}}$) [16] presented as relative deviations *RD*s ($RD/\% = 100 \cdot (C_{p,\text{this work}} - C_{p,\text{lit}})/C_{p,\text{this work}}$).

The isentropic compressibility, κ_S, was determined from Equation (5) using the experimental speed of sound and determined density. The results are collected in Table 7. The overall expanded uncertainty of κ_S was estimated to be $U(\kappa_S) = 1.5 \cdot 10^{-3} \kappa_S$ Pa^{-1}. The isentropic compressibility calculated from the speed of sound and density reported by Plantier et al. [15] is in an excellent agreement with those reported in this work. The *RD*s are in the range from −0.31% to 0.16% (see Figure 6), the *AARD* is 0.16%. The *RD*s between κ_S obtained from $p\rho T$ data reported by Safarov et al. [16] and obtained in this work are in the range from −0.004% to 6.3% (see Figure 6), the *AARD* is 2.1%.

Table 7. The isentropic compressibility, κ_S, of 1-butanol at pressures up to 100 MPa and within the temperature range from (293 to 318) K.

p (MPa)	$\kappa_S \cdot 10^9$ (Pa^{-1})					
	T (K)					
	293.15	298.15	303.15	308.15	313.15	318.15
0.1	0.7826	0.8080	0.8345	0.8621	0.8909	0.9209
10	0.7150	0.7361	0.7579	0.7805	0.8038	0.8279
20	0.6586	0.6765	0.6949	0.7138	0.7332	0.7532
30	0.6117	0.6272	0.6430	0.6592	0.6757	0.6926
40	0.5720	0.5855	0.5994	0.6134	0.6278	0.6423
50	0.5379	0.5499	0.5622	0.5746	0.5872	0.5999
60	0.5083	0.5191	0.5300	0.5411	0.5523	0.5636
70	0.4823	0.4920	0.5019	0.5119	0.5219	0.5321
80	0.4592	0.4681	0.4771	0.4861	0.4952	0.5044
90	0.4387	0.4468	0.4550	0.4633	0.4716	0.4799
100	0.4202	0.4277	0.4353	0.4428	0.4504	0.4580

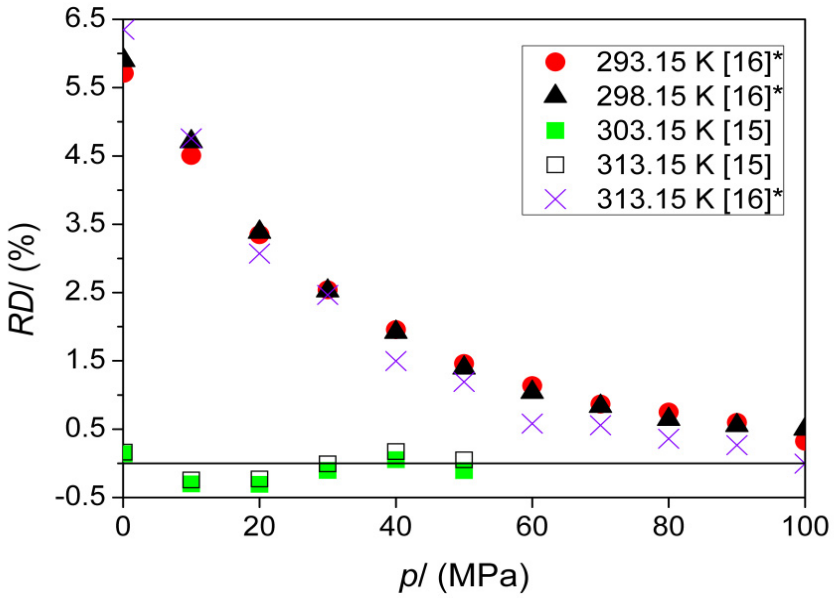

Figure 6. Comparison of the isentropic compressibility of 1-butanol as a function of pressure obtained in this work ($\kappa_{S,\text{this work}}$) with the literature values ($\kappa_{S,\text{lit}}$) [15,16] presented as relative deviations *RD*s ($RD/\% = 100\cdot(\kappa_{S,\text{this work}} - \kappa_{S,\text{lit}})/\kappa_{S,\text{this work}}$); * calculated from the $p\rho T$ data [16].

Based on the temperature dependence of density, the isobaric thermal expansion was calculated using a definition (Equation (4)). The obtained results are collected in Table 8. The overall expanded uncertainty of α_p is $U(\alpha_p) = 1\cdot10^{-2}\alpha_p$ K^{-1}. The agreement with literature data is very good, the *RDs* are in the range from −1.9 to 0.17% [16] and from −2.2 to 0.19% [17] (see Figure 7). The *AARD* is 0.83% [16] and 1.0% [17].

Table 8. The isobaric thermal expansion, α_p, of 1-butanol at pressures up to 100 MPa and within the temperature range from (293 to 318) K.

p (MPa)	$\alpha_p\cdot10^3$ (K^{-1})					
	T (K)					
	293.15	298.15	303.15	308.15	313.15	318.15
0.1	0.931	0.945	0.959	0.973	0.988	1.002
10	0.879	0.891	0.903	0.915	0.928	0.941
20	0.834	0.845	0.856	0.868	0.879	0.890
30	0.796	0.806	0.817	0.827	0.837	0.848
40	0.763	0.772	0.782	0.792	0.802	0.812
50	0.733	0.742	0.752	0.761	0.770	0.780
60	0.707	0.715	0.724	0.733	0.742	0.751
70	0.682	0.691	0.699	0.708	0.717	0.726
80	0.660	0.668	0.677	0.686	0.694	0.703
90	0.640	0.648	0.656	0.665	0.673	0.682
100	0.621	0.629	0.637	0.646	0.654	0.663

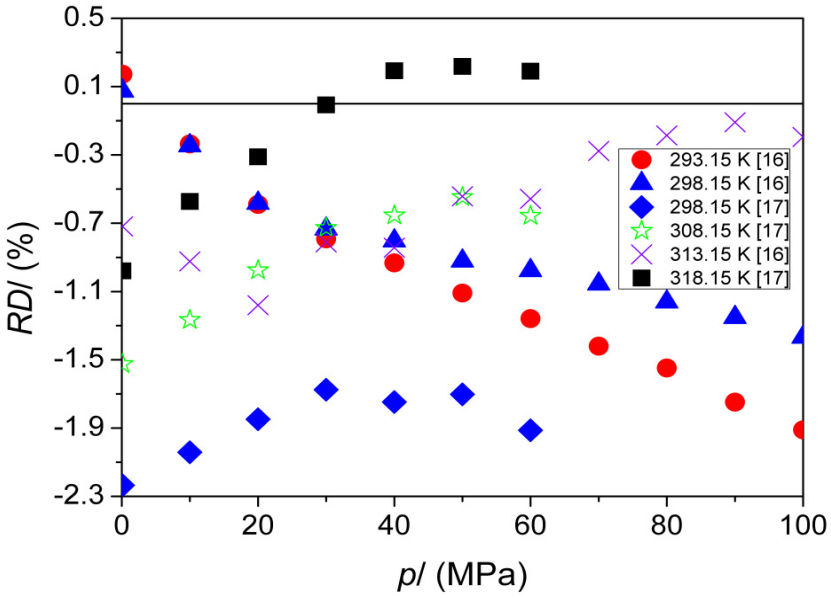

Figure 7. Comparison of the isobaric thermal expansion of 1-butanol as a function of pressure obtained in this work ($\alpha_{p,\text{this work}}$) with the literature values ($\alpha_{p,\text{lit}}$) [16,17] presented as relative deviations *RD*s ($RD/\% = 100 \cdot (\alpha_{p,\text{this work}} - \alpha_{p,\text{lit}})/\alpha_{p,\text{this work}}$).

For the comprehensive characterization of the tested liquid, the compressibility at a constant temperature, κ_T, is the next important material constant. In this work, κ_T was calculated from κ_S using Eq. (3), the results are listed in Table 9. The overall expanded uncertainty of κ_T was estimated to be $U(\kappa_T) = 5 \cdot 10^{-3} \kappa_T$ Pa^{-1}. In this work, the κ_T was obtained by the acoustic method based on integration procedures. On the other hand, the κ_T obtained by the densimetric method is based on differentiation procedures [16,17]. The *RD*s between results obtained in this work using the acoustic method and literature data obtained using the densimetric method are in the range from −0.08 to 5.2% [16] and from −3.5 to −1.5% [17] (see Figure 8). The *AARD* is 1.6% [16] and 2.7% [17].

Table 9. The isothermal compressibility, κ_T, of 1-butanol at pressures up to 100 MPa and within the temperature range from (293 to 318) K.

***p* (MPa)**	**$\kappa_T \cdot 10^9$ (Pa^{-1})**					
	***T* (K)**					
	293.15	298.15	303.15	308.15	313.15	318.15
0.1	0.917	0.946	0.977	1.009	1.042	1.077
10	0.834	0.858	0.884	0.910	0.937	0.964
20	0.766	0.786	0.808	0.830	0.852	0.875
30	0.709	0.727	0.745	0.764	0.783	0.803
40	0.661	0.677	0.693	0.709	0.726	0.743
50	0.620	0.634	0.648	0.663	0.677	0.692
60	0.584	0.597	0.610	0.623	0.636	0.649
70	0.553	0.564	0.576	0.588	0.600	0.612
80	0.525	0.536	0.546	0.557	0.568	0.579
90	0.500	0.510	0.520	0.530	0.540	0.550
100	0.478	0.487	0.496	0.506	0.515	0.524

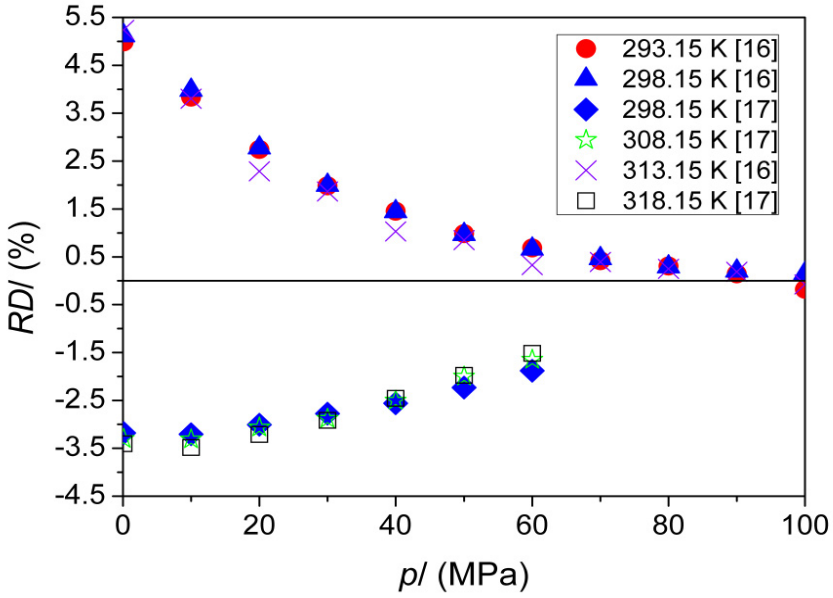

Figure 8. Comparison of the isothermal compressibility of 1-butanol as a function of pressure obtained in this work ($\kappa_{T,\text{this work}}$) with the literature values ($\kappa_{T,\text{lit}}$) [16,17] presented as relative deviations *RD*s ($RD/\% = 100\cdot(\kappa_{T,\text{this work}} - \kappa_{T,\text{lit}})/\kappa_{T,\text{this work}}$).

The molar isochoric heat capacity, C_V, was calculated using the experimental speed of sound as well as the determined density, molar isobaric heat capacity and isobaric thermal expansion:

$$C_V = C_p - \frac{\alpha_p^2 \cdot T \cdot V}{\frac{1}{\rho \cdot u^2} + \frac{\alpha_p^2 \cdot T \cdot V}{C_p}}. \quad (10)$$

The C_V values obtained in this work are collected in Table 10. The overall expanded uncertainty of C_V was estimated to be $U(C_V) = 2\cdot10^{-2}C_V$ J·mol^{-1}·K^{-1}. The C_V values obtained in this work by the acoustic method and those obtained using the densimetric method by Safarov et al. [16] are in excellent agreement. The *RD*s are in the range from −0.19 to 1.1% [16] (see Figure 9) and *AARD* is 0.35% [16].

Table 10. The isochoric molar heat capacity, C_V, of 1-butanol at pressures up to 100 MPa and within the temperature range from (293 K to 318) K.

***p* (MPa)**	***C*$_V$ (J·mol^{-1}·K^{-1})**					
	***T* (K)**					
	293.15	298.15	303.15	308.15	313.15	318.15
0.1	148.3	151.3	154.4	157.8	161.2	164.8
10	148.2	151.1	154.2	157.5	160.9	164.4
20	148.0	150.9	154.0	157.2	160.6	164.1
30	147.8	150.7	153.8	157.0	160.3	163.7
40	147.7	150.6	153.6	156.7	160.0	163.4
50	147.6	150.4	153.4	156.5	159.7	163.1
60	147.4	150.2	153.2	156.3	159.5	162.8
70	147.3	150.1	153.0	156.1	159.2	162.5
80	147.2	150.0	152.8	155.9	159.0	162.2
90	147.1	149.8	152.7	155.6	158.7	162.0
100	147.0	149.7	152.5	155.4	158.5	161.7

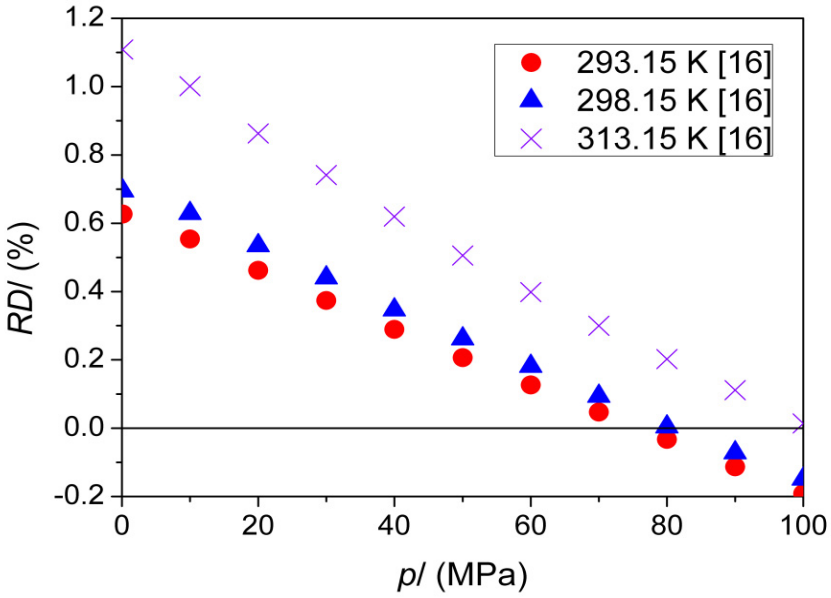

Figure 9. Comparison of the isochoric heat capacity of 1-butanol as a function of pressure obtained in this work ($C_{V,\text{this work}}$) with the literature values ($C_{V,\text{lit}}$) [16] presented as relative deviations *RD*s ($RD/\% = 100 \cdot (C_{V,\text{this work}} - C_{V,\text{lit}})/C_{V,\text{this work}}$).

The internal pressure was calculated using the experimental speed of sound and determined density, isobaric heat capacity, and isobaric thermal expansion:

$$p_{\text{int}} = T \cdot \left(\frac{\alpha_p}{\kappa_T}\right) - p = \left[T \cdot \alpha_p \cdot \left(\frac{1}{\rho \cdot u^2} + \frac{\alpha_p^2 \cdot T \cdot V}{C_p}\right)^{-1}\right] - p. \quad (11)$$

The results are collected in Table 11. The overall expanded uncertainty of p_{int} was estimated to be $U(p_{\text{int}}) = 1 \cdot 10^{-2} p_{\text{int}}$ Pa. The *RD*s for p_{int} obtained in this work by the acoustic method and those obtained by the densimetric method are in the range from −6.3 to −0.36% [16] and from −0.21 to 3.0% [17] (see Figure 10). The *AARD* is 2.7% [16] and 1.7% [17].

Table 11. The internal pressure, p_{int}, of 1-butanol at pressures up to 100 MPa and within the temperature range from (293 to 318) K.

p (MPa)	$p_{\text{int}} \cdot 10^{-6}$ (Pa)					
	T (K)					
	293.15	298.15	303.15	308.15	313.15	318.15
0.1	297.9	297.4	297.2	296.9	296.5	295.9
10	299.1	299.4	299.7	300.0	300.2	300.5
20	299.6	300.5	301.4	302.2	303.0	303.7
30	299.4	300.8	302.2	303.6	304.9	306.1
40	298.5	300.4	302.2	304.0	305.8	307.6
50	296.9	299.2	301.5	303.8	306.0	308.3
60	294.6	297.4	300.1	302.8	305.5	308.3
70	291.8	295.0	298.1	301.3	304.4	307.6
80	288.5	292.0	295.6	299.2	302.8	306.4
90	284.7	288.6	292.6	296.6	300.6	304.7
100	280.5	284.8	289.2	293.6	298.0	302.5

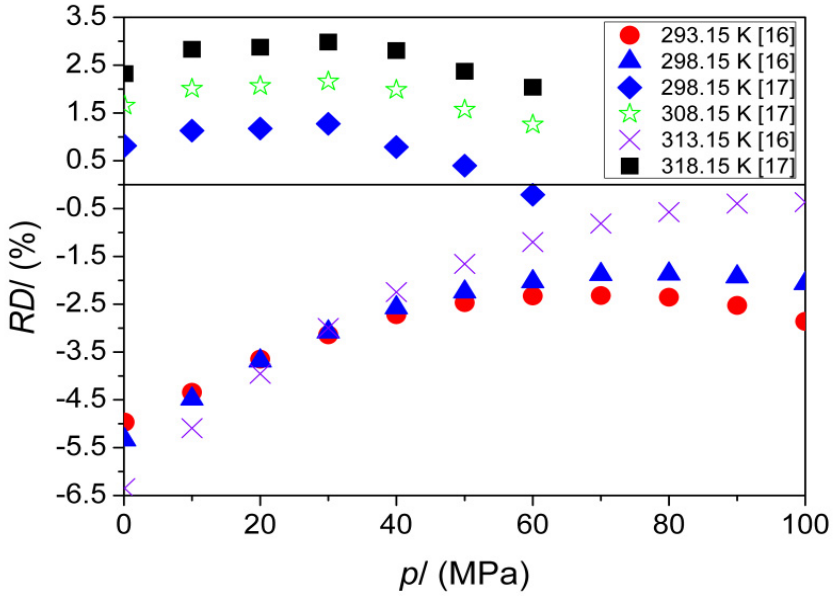

Figure 10. Comparison of the internal pressure of 1-butanol as a function of pressure obtained in this work ($p_{\text{int,this work}}$) with the literature values ($p_{\text{int,lit}}$) [16,17] presented as relative deviations *RD*s ($RD/\% = 100 \cdot (p_{\text{int,this work}} - p_{\text{int,lit}})/p_{\text{int,this work}}$).

The relative deviations *RD*s (Figure 10) suggest that the pressure dependence of the internal pressure of 1-butanol is different depending on the data source (see Figure 11).

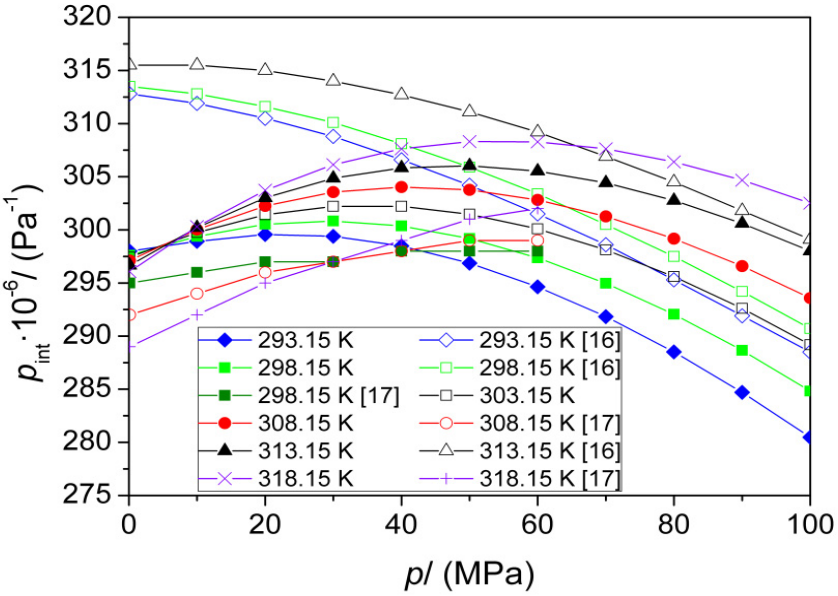

Figure 11. Comparison of the internal pressure of 1-butanol as a function of pressure obtained in this work with those obtained from the $p\rho T$ literature data [16,17].

The density, isentropic compressibility and isobaric thermal expansion of 1-butanol were compared with density, isentropic compressibility and isobaric thermal expansion of heptane [36,37], ethanol [36,37], dodecane [38], diesel oil (ekodiesel ultra) [12] and biodiesel [12]. Heptane and dodecane are components of the fuels [36–38]. The engine simulations were carried out first using heptane and then dodecane as a more suitable "low or no sulphur", "ideal" surrogate component for petrodiesel fuels [39,40]. Moreover, the thermophysical properties of dodecane are similar to the thermophysical properties of aviation kerosene [41]. For comparison, ethanol was also chosen as the most commonly

used bioalcohol. Additionally, the properties of 1-butanol were compared with those of petrodiesel oil with sulfur content < 10 mg/kg which fulfilled norm EN 590 [12] (named ekodiesel ultra) and biodiesel composed of fatty acid methyl esters from rapeseed oil, which fulfilled norm EN 14214 [12]. Among studied fuel components, the density of 1-butanol at 288.15 K is the closest to norm EN 590 for diesel and the most similar to the density of diesel oil ekodiesel ultra (see Figure 12). Moreover, the differences between the density of 1-butanol and ekodiesel ultra decrease with increasing pressure from 2.8% at 0.1 MPa to 1.9% at 100 MPa and at 298.15 K (see Figure 13).

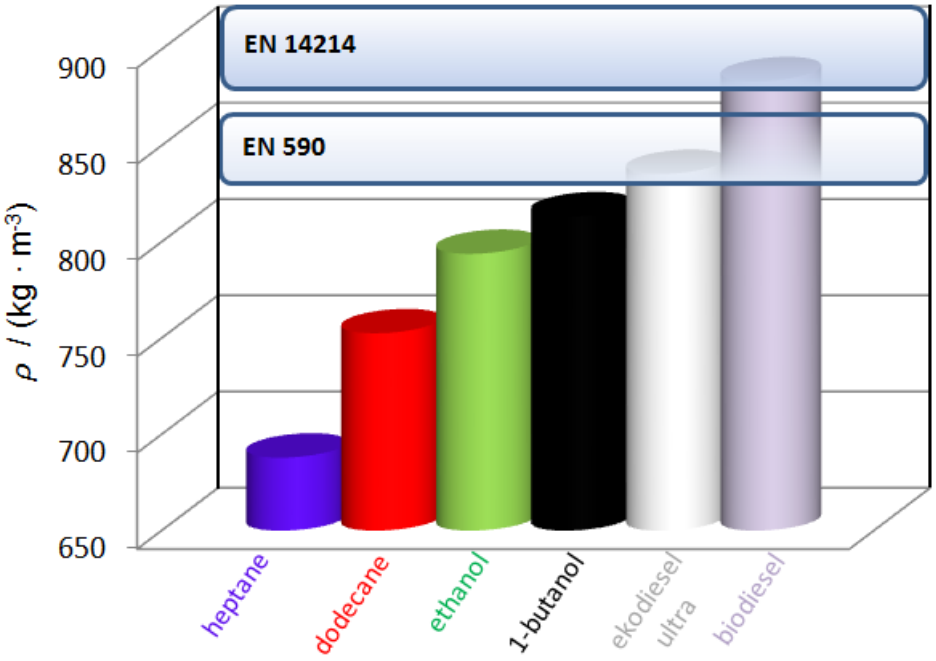

Figure 12. Comparison of the density at 288.15 K of heptane [36,37], dodecane [38], ethanol [36,37], 1-butanol (this work), ekodiesel ultra [12], biodiesel [12] with norm EN 590 for diesel and EN 14214 for biodiesel.

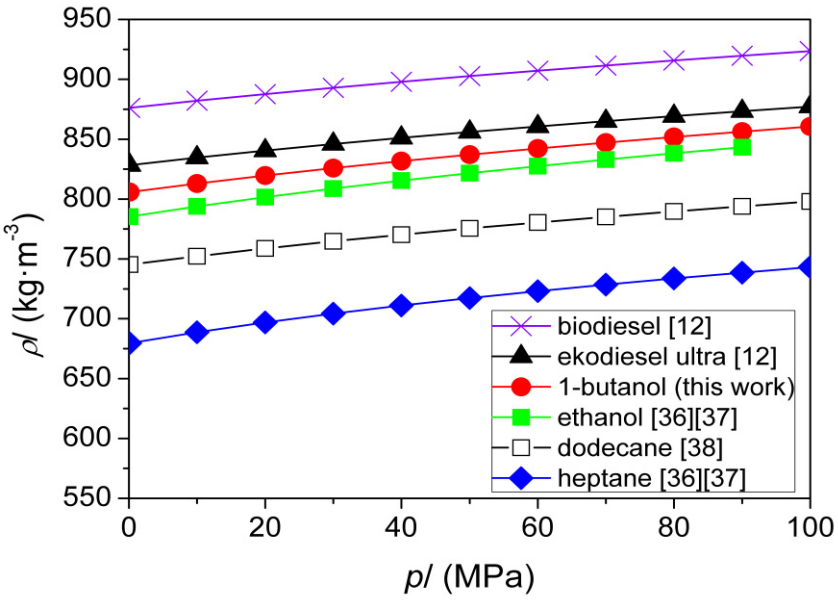

Figure 13. The pressure dependence of density of heptane and dodecane—fuel components, ethanol—the most common used bioalcohol, low sulfur diesel oil (ekodiesel ultra) and biodiesel (FAME) at 298.15 K.

The 1-butanol is less compressible than heptane by 43 ÷ 20% in the pressure range of 0.1 ÷ 100 MPa, and ethanol by 21 ÷ 12% in the pressure range of 0.1 ÷ 90 MPa at 298.15 K. The 1-butanol is more compressible than diesel by 18 ÷ 12% and biodiesel by 28 ÷ 17% in the pressure range of 0.1 ÷ 100 MPa at 298.15 K. On the other hand, the compressibility of 1-butanol is close to dodecane, and furthermore, the differences between compressibility of 1-butanol and dodecane decrease with increasing pressure from 1.5% at 0.1 MPa to 0.5% at 100 MPa and at 298.15 K (Figure 14).

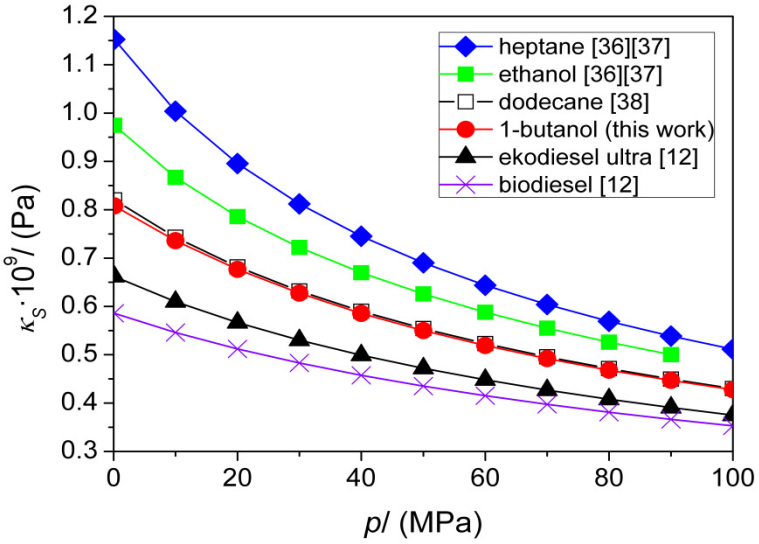

Figure 14. The pressure dependence of isentropic compressibility of heptane and dodecane—fuel components, ethanol—the most common used bioalcohol, low sulfur diesel oil (ekodiesel ultra) and biodiesel (FAME) at 298.15 K.

As in the case of isentropic compressibility, the isobaric thermal expansion of 1-butanol is lower than those of heptane by 32 ÷ 15% in the pressure range of 0.1 ÷ 100 MPa, and ethanol 15 ÷ 12% in the pressure range of 0.1 ÷ 90 MPa at 298.15 K. The isobaric thermal expansion of 1-butanol is higher than those of diesel by 10 ÷ 7% and biodiesel by 12 ÷ 5% in the pressure range of 0.1 ÷ 100 MPa at 298.15 K. On the other hand, isobaric thermal expansion of 1-butanol is the most similar to dodecane and likewise, the pressure dependence of isobaric thermal expansion of 1-butanol is the most similar to the pressure dependence of isobaric thermal expansion of dodecane (Figure 15). The differences between the expansivity of 1-butanol and dodecane slightly decrease with increasing pressure from 3.3% at 0.1 MPa to 2.9% at 100 MPa and at 298.15 K.

The internal pressure is related to the solubility parameter [42–48] and cohesive energy density [43,46,49]. According to the definition, the internal pressure reflects molecular interactions which determine the change of internal energy that accompanying a very small isothermal expansion of 1 mole of liquid. Therefore, the internal pressure should be affected mainly by dispersion, repulsion, and weak dipole–dipole interactions. Kartsev et al. [50–53] pointed out that the temperature dependence of internal pressure is sensitive to the structural organization and reflects the character of the interactions of not hydrogen-bonded, hydrogen-bonded with the spatial net of H-bonds and associated liquids. They showed that, at atmospheric pressure, the sign reversal of the temperature coefficient of the internal pressure from $(\partial p_{int}/\partial T)_p > 0$ to $(\partial p_{int}/\partial T)_p < 0$ is characteristic for primary linear alkanols. Our group found that the pressure coefficient of internal pressure $(\partial p_{int}/\partial p)_T$is also sensitive to the structural organization of the molecular liquids like alcohols [20,54,55] as well as ionic liquids [56] and reflects the character of the interactions. The temperature and pressure dependence of the internal pressure of 1-butanol found in this work confirms the results obtained previously for 1-alkanols [20,54,55]. In the temperature and pressure ranges under investigation, the maximum of the pressure dependence of the internal pressure of 1-butanol was observed for each isotherm

(see Figure 16). With increasing temperature, the maximum moves toward higher pressures. Thus, the internal pressure first increases with increasing pressure and then it decreases. This was also observed for ethanol and for other 1-alkanols from 1-pentanol to 1-decanol [20,54,55]. The internal pressure of 1-butanol obtained by Safarov et al. [16] decreases with increasing pressure ($(\partial p_{int}/\partial p)_T < 0$) in the pressure range under investigation and at temperatures as in this work. Meanwhile, the internal pressure of 1-butanol obtained by Dávila et al. [17] increases with increasing pressure ($(\partial p_{int}/\partial p)_T > 0$) in the pressure range under investigation and at temperatures as in this work. Moreover, the results obtained in this work shows that with the increasing pressure, the temperature dependence of the internal pressure of 1-butanol changes from $(\partial p_{int}/\partial T)_p < 0$ to $(\partial p_{nt}/\partial T)_p > 0$. This reflects the crossing point of the isotherms of the internal pressure, which was observed for ethanol and for other 1-alkanols from 1-pentanol to 1-decanol [20,54,55]. Dávila et al. [17] also found the crossing point of internal pressure isotherms of 1-butanol. On the other hand, Safarov et al. [16] did not observe this effect; $(\partial p_{int}/\partial T)_p > 0$ in the whole pressure range. The inspection of literature data shows better internal coherence of $p_{int}(p,T)$ dependence obtained by the acoustic method than obtained by the densimetric method. In the case of the densimetric method, isobaric thermal expansion and isothermal compressibility are obtained by differentiation using their definitions acquired by Equations (4) and (6), respectively. Meanwhile, in the acoustic method, differentiation is needed only for the determination of isobaric thermal expansion (Equation (4)). The crossing point of the internal pressure isotherms was also observed for 2-methyl-2-butanol and 3-pentanol [54,55]. For 3-pentanol, the crossing point of each two neighbor isotherms shifts toward higher pressure with increasing temperature [54,55]. For 2-methyl-2-butanol, the crossing point of each two neighbor isotherms appears at temperatures higher than 303.15 K and it moves toward higher pressure with increasing temperature as in the case of 3-pentanol [55]. On the other hand, for 2-methyl-1-butanol, the crossing point is not observed, and the internal pressure increases with increasing temperature over the whole investigated temperature and pressure range. However, the temperature dependence of the internal pressure of 2-methyl-1-butanol under atmospheric pressure indicates that the crossing point could appear at higher temperatures [55].

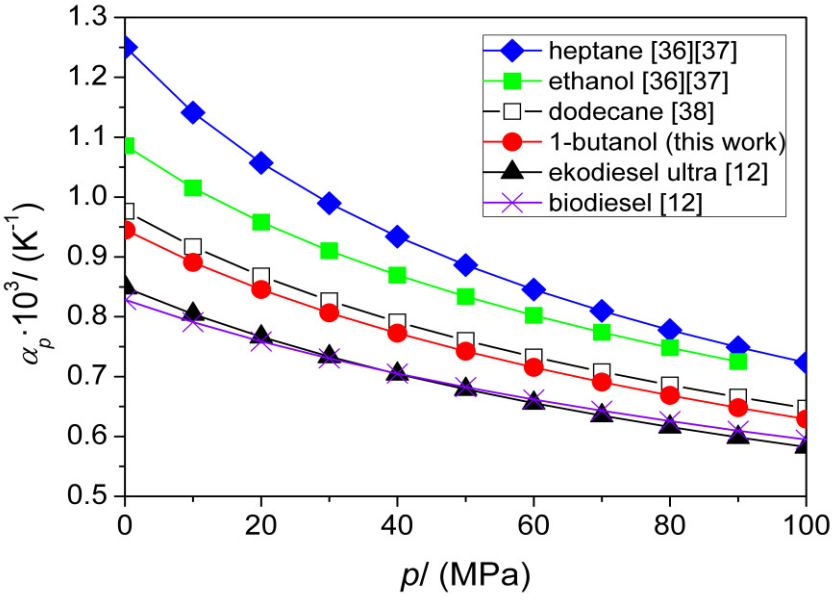

Figure 15. The pressure dependence of isobaric thermal expansion of heptane and dodecane—fuel components, ethanol—the most common used bioalcohol, low sulfur diesel oil (ekodiesel ultra) and biodiesel (FAME) at 298.15 K.

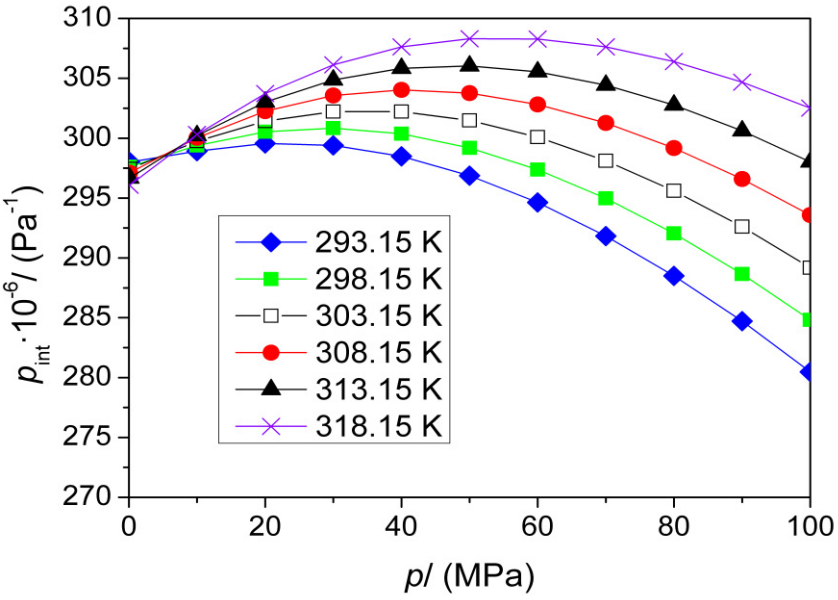

Figure 16. The pressure dependence of internal pressure of 1-butanol obtained in this work.

4. Summary

The speed of sound in 1-butanol was conducted in the temperature range from (293 to 318) K and at pressures up to 101 MPa. The density of the liquid under test was measured within the temperatures from (293 to 318) K under atmospheric pressure. From the experimental results, the pressure and temperature dependence of the density, isobaric heat capacity and related thermodynamic properties such as isentropic and isothermal compressibilities, the isobaric thermal expansion and internal pressure as a function of temperature and pressure were determined using the acoustic method. The obtained results show that the density of 1-butanol is close to norm EN 590 for diesel oil and, as a consequence, is close to the density of ekodiesel ultra. The isobaric expansivity and isentropic compressibility of 1-butanol are close to those of dodecane—a surrogate component for petrodiesel fuels and aviation kerosene. The temperature and pressure dependence of the internal pressure, obtained by the acoustic method, qualitatively confirms similarities and dissimilarities of 1-butanol, other 1-alkanols as well as 2-methyl-2-butanol and 3-pentanol. Discrepancies in the sign of $(\partial p_{int}/\partial T)_p$ and $(\partial p_{int}/\partial p)_T$ were found for 1-butanol obtained by the acoustic method and densimetric method. Thus, the determination of internal pressure as a function of temperature and pressure is still an open, complex issue.

Author Contributions: M.D. conceived and designed the research, conducted the experimental research, analyzed the data, wrote the manuscript. All authors have read and agreed to the published version of the manuscript.

Funding: The work was financed by a statutory activity subsidy from the Polish Ministry of Science and Higher Education for the Institute of Chemistry of University of Silesia in Katowice.

Conflicts of Interest: The author declare no conflict of interest.

References

1. Salleh, M.S.M.; Ibrahim, M.F.; Roslan, A.M.; Abd-Aziz, S. Improved biobutanol production in 2-L simultaneous saccharification and fermentation with delayed yeast extract feeding and in-situ recovery. *Sci. Rep.* **2019**, *9*, 7443. [CrossRef] [PubMed]
2. Tucki, K.; Orynycz, O.; Wasiak, A.; Świć, A.; Mruk, R.; Botwińska, K. Estimation of carbon dioxide emissions from a diesel engine powered by lignocellulose derived fuel for better management of fuel production. *Energies* **2020**, *13*, 561. [CrossRef]
3. Meng, L.; Zeng, C.; Li, Y.; Nithyanandan, K.; Lee, T.H.; Lee, C. An experimental study on the potential usage of acetone as an oxygenate additive in PFI SI engines. *Energies* **2016**, *9*, 256. [CrossRef]

4. Rodríguez-Fernández, J.; Hernández, J.J.; Calle-Asensio, A.; Ramos, Á.; Barba, J. Selection of blends of diesel fuel and advanced biofuels based on their physical and thermochemical properties. *Energies* **2019**, *12*, 2034. [CrossRef]
5. Kamiński, W.; Tomczak, E.; Górak, A. Biobutanol—Production and purification methods. *Atmosphere* **2011**, *2*, 3.
6. Gan, L.; Chidambaram, A.; Fonquernie, P.G.; Light, M.E.; Choquesillo-Lazarte, D.; Huang, H.; Solano, E.; Fraile, J.; Viñas, C.; Teixidor, F.; et al. A highly water-stable meta-carborane-based copper metal—Organic framework for efficient high-temperature butanol separation. *J. Am. Chem. Soc.* **2020**, *142*, 8299–8311. [CrossRef] [PubMed]
7. Azambuja, S.P.H.; Goldbeck, R. Butanol production by *Saccharomyces cerevisiae*: Perspectives, strategies and challenges. *World J. Microbiol. Biotechnol.* **2020**, *36*, 48. [CrossRef] [PubMed]
8. Li, S.; Huang, L.; Ke, C.; Pang, Z.; Liu, L. Pathway dissection, regulation, engineering and application: Lessons learned from biobutanol production by solventogenic clostridia. *Biotechnol. Biofuels* **2020**, *13*, 39. [CrossRef] [PubMed]
9. Qureshi, N.; Lin, X.; Liu, S.; Saha, B.C.; Mariano, A.P.; Polaina, J.; Ezeji, T.C.; Friedl, A.; Maddox, I.S.; Klasson, K.T.; et al. Global view of biofuel butanol and economics of its production by fermentation from sweet sorghum bagasse, food waste, and yellow top presscake: Application of novel technologies. *Fermentation* **2020**, *6*, 58. [CrossRef]
10. El-Dalatony, M.M.; Salama, E.-S.; Kurade, M.B.; Hassan, S.H.A.; Oh, S.-E.; Kim, S.; Jeon, B.-H. Utilization of microalgal biofractions for bioethanol, higher alcohols, and biodiesel production: A review. *Energies* **2017**, *10*, 2110. [CrossRef]
11. Mahmud, N.; Rosentrater, K.A. Life-cycle assessment (LCA) of different pretreatment and product separation technologies for butanol bioprocessing from oil palm frond. *Energies* **2020**, *13*, 155. [CrossRef]
12. Dzida, M.; Prusakiewicz, P. The effect of temperature and pressure on the physicochemical properties of petroleum diesel oil and biodiesel fuel. *Fuel* **2008**, *87*, 1941–1948. [CrossRef]
13. Oakley, B.A.; Barber, G.; Worden, T.; Hanna, D. Ultrasonic parameters as a function of absolute hydrostatic pressure. I. A review of the data for organic liquids. *J. Phys. Chem. Ref. Data* **2003**, *32*, 1501–1533. [CrossRef]
14. Khasanshin, T.S. Sonic velocity in liquid primary normal alcohols. *Teplofiz. Vys. Temp.* **1991**, *29*, 710–716.
15. Plantier, F.; Daridon, J.L.; Lagourette, B. Nonlinear parameter (*B/A*) measurements in methanol, 1-butanol and 1-octanol for different pressures and temperatures. *J. Phys. D Appl. Phys.* **2002**, *35*, 1063–1067. [CrossRef]
16. Safarov, J.; Ahmadov, B.; Mirzayev, S.; Shahverdiyev, A.; Hassel, E.P. Thermophysical properties of 1-butanol over a wide range of temperatures and pressures up to 200 Mpa. *J. Mol. Liq.* **2015**, *209*, 465–479. [CrossRef]
17. Dávila, M.J.; Alcalde, R.; Atilhan, M.; Aparicio, S. PρT measurements and derived properties of liquid 1-alkanols. *J. Chem. Thermodyn.* **2012**, *47*, 241–259. [CrossRef]
18. Khasanshin, T.S. "Structure-property" quantitative correlations for the density of primary normal alcohols. *Teplofiz. Vys. Temp.* **1997**, *35*, 886–895.
19. Cibulka, I.; Ziková, M. Liquid densities at elevated pressures of 1-alkanols from C_1 to C_{10}: A critical evaluation of experimental data. *J. Chem. Eng. Data* **1994**, *39*, 876–886. [CrossRef]
20. Dzida, M. Speeds of sound, densities, isobaric thermal expansion, compressibilities and internal pressures of heptan-1-ol, octan-1-ol, nonan-1-ol and decan-1-ol at temperatures from (293 to 318) K and pressures up to 100 MPa. *J. Chem. Eng. Data* **2007**, *52*, 521–531. [CrossRef]
21. Dzida, M. Study of the effects of temperature and pressure on the thermodynamic and acoustic properties of pentan-1-ol, 2-methyl-2-butanol, and cyclopentanol in the pressure range from (0.1 to 100) MPa and temperature from (293 to 318) K. *J. Chem. Eng. Data* **2009**, *54*, 1034–1040. [CrossRef]
22. Zábranský, M.; Růžička, V.; Majer, V. Heat Capacities of Organic Compounds in Liquid State. I. C1 to C18 1-Alkanols. *J. Phys. Chem. Ref. Data* **1990**, *19*, 719–762. [CrossRef]
23. Davis, L.A.; Gordon, R.B. Compression of mercury at high pressure. *J. Chem. Phys.* **1967**, *46*, 2650–2660. [CrossRef]
24. Sun, T.F.; Seldam, C.A.T.; Kortbeek, P.J.; Trappeniers, N.J.; Biswas, S.N. Acoustic and Thermodynamic Properties of ethanol from 273.15 to 333.1 5 K and up to 280 MPa. *Phys. Chem. Liq.* **1988**, *18*, 107–116. [CrossRef]
25. Zorębski, E.; Dec, E. Speeds of sound and isentropic compressibilities for binary mixtures of 1,2-ethanediol with 1-butanol, 1-hexanol, or 1-octanol in the temperature range from 293.15 to 313.15 K. *J. Mol. Liq.* **2012**, *168*, 61–68. [CrossRef]

26. Outcalt, S.L.; Laesecke, A.; Fortin, T.J. Density and speed of sound measurements of 1- and 2-butanol. *J. Mol. Liq.* **2010**, *151*, 50–59. [CrossRef]
27. Cristino, A.F.; Nobre, L.C.S.; Bioucas, F.E.B.; Santos, Â.F.S.; de Castro, C.A.N.; Lampreia, I.M.S. Volumetric and sound speed study of aqueous 1-butanol liquid mixtures at different temperatures. *J. Chem. Thermodyn.* **2019**, *134*, 127–135. [CrossRef]
28. Gascón, I.; Martin, S.; Cea, P.; López, M.C.; Royo, F.M. Density and speed of sound for binary mixtures of a cyclic ether with a butanol isomer. *J. Sol. Chem.* **2002**, *31*, 905–916. [CrossRef]
29. Troncoso, J.; Tovar, C.A.; Cerdeiriña, C.A.; Carballo, E.; Romaní, L. Temperature dependence of densities and speeds of sound of nitromethane + butanol isomers in the range (288.15−308.15) K. *J. Chem. Eng. Data* **2001**, *46*, 312–316. [CrossRef]
30. Zorębski, E.; Geppert-Rybczyńska, M. Thermodynamic and transport properties of (1-Butanol +1,4-Butanediol) at temperatures from (298.15 to 318.15) K. *J. Chem. Thermodyn.* **2010**, *42*, 409–418. [CrossRef]
31. Kiyohara, O.; Benson, G.C. Ultrasonic speeds and isentropic compressibilities of n-alkanol + n-heptane mixtures at 298.15 K. *J. Chem. Thermodyn.* **1979**, *11*, 861–873. [CrossRef]
32. Troncoso, J.; Carballo, E.; Cerdeiriña, C.A.; González, D.; Romaní, L. Systematic determination of densities and speeds of sound of nitroethane + isomers of butanol in the range (283.15–308.15) K. *J. Chem. Eng. Data* **2000**, *45*, 594–599. [CrossRef]
33. Żak, A.; Dzida, M.; Zorębski, M.; Ernst, S. A high pressure system for measurements of the speed of sound in liquids. *Rev. Sci. Instrum.* **2000**, *71*, 1756–1765. [CrossRef]
34. Zúñiga-Moreno, A.Z.; Galicia-Luna, L.A.; Camacho-Camacho, L.E. Compressed liquid densities of 1-butanol and 2-butanol at temperatures from 313 K to 363 K and pressures up to 25 MPa. *J. Chem. Thermodyn.* **2007**, *39*, 254–260. [CrossRef]
35. Musiał, M.; Zorębski, M.; Dzida, M.; Safarov, J.; Zorębski, E.; Hassel, E. High pressure speed of sound and related properties of 1-ethyl-3-methylimidazolium methanesulfonate. *J. Mol. Liq.* **2019**, *276*, 885–896. [CrossRef]
36. Dzida, M.; Żak, A.; Ernst, S. Thermodynamic and acoustic properties of binary mixtures of alcohols and alkanes. I. Speed of sound in (ethanol + *n*-heptane) under elevated pressures. *J. Chem. Thermodyn.* **2005**, *37*, 405–414. [CrossRef]
37. Dzida, M.; Marczak, W. Thermodynamic and acoustic properties of binary mixtures of alcohols and alkanes. II. Density and heat capacity of (ethanol + *n*-heptane) under elevated pressures. *J. Chem. Thermodyn.* **2005**, *37*, 826–836. [CrossRef]
38. Dzida, M.; Cempa, M. Thermodynamic and acoustic properties of (heptane + dodecane) mixtures under elevated pressures. *J. Chem. Thermodyn.* **2008**, *40*, 1531–1541. [CrossRef]
39. Knothe, G.; Sharp, C.A.; Ryan, T.W. Exhaust emissions of biodiesel, petrodiesel, neat methyl esters, and alkanes in a new technology engine. *Energy Fuels* **2006**, *20*, 403–408. [CrossRef]
40. Luo, Z.; Som, S.; Sarathy, S.M.; Plomer, M.; Pitz, W.J.; Longman, D.E.; Lu, T. Development and validation of an n-dodecane skeletal mechanism for spray combustion applications. *Comb. Theory Model.* **2014**, *18*, 187–203. [CrossRef]
41. Lemmon, E.W.; Huber, M.L. Thermodynamic properties of *n*-dodecane. *Energy Fuels* **2004**, *18*, 960–967. [CrossRef]
42. Hildebrand, J.H. Theory of solubility. *Phys. Rev.* **1923**, *21*, 46–52. [CrossRef]
43. Hildebrand, J.H.; Prausnitz, J.M.; Scott, R.L. *Regular and Related Solutions*; Van Nostrand-Reinhold: Princeton, NJ, USA, 1970.
44. Barton, A.F.M. Solubility parameters. *Chem. Rev.* **1975**, *75*, 731–753. [CrossRef]
45. Dack, M.R.J. The importance of solvent internal pressure and cohesion to solution phenomena. *Chem. Soc. Rev.* **1975**, *4*, 211–229. [CrossRef]
46. Dack, M.R.J. Solvent structure. The use of internal pressure and cohesive energy density to examine contributions to solvent-solvent interactions. *Aust. J. Chem.* **1975**, *28*, 1643–1648. [CrossRef]
47. Verdier, S.; Andersen, S.I. Internal pressure and solubility parameter as a function of pressure. *Fluid Phase Equlib.* **2005**, *231*, 125–137. [CrossRef]
48. Bagley, E.B.; Nelson, T.P.; Scigliano, J.M. Three-dimensional solubility parameters and their relation to internal pressure measurements in polar and hydrogen bonding solvents. *J. Paint Technol.* **1971**, *43*, 35–42.

49. Allen, G.; Gee, G.; Wilson, G.J. Intermolecular forces and chain flexibilities in polymers: I. Internal pressures and cohesive energy densities of simple liquids. *Polymer* **1960**, *1*, 456–466. [CrossRef]
50. Kartsev, V.N.; Rodnikova, M.N.; Bartel, I.; Shtykov, S.N. The temperature dependence of internal pressure in liquids. *Rus. J. Phys. Chem.* **2002**, *76*, 903–905.
51. Kartsev, V.N.; Rodnikova, M.N.; Shtykov, S.N. Inversion of the temperature coefficient of internal pressure and structural organization of liquid phase systems. *J. Struct. Chem.* **2004**, *45*, 91–95. [CrossRef]
52. Kartsev, V.N.; Rodnikova, M.N.; Shtykov, S.N. On internal pressure, its temperature dependence, and the structure of liquid-phase systems. *J. Struct. Chem.* **2004**, *45*, 96–99. [CrossRef]
53. Kartsev, V.N. To the understanding of the structural sensitivity of the temperature coefficient of internal pressure. *J. Struct. Chem.* **2004**, *45*, 832–837. [CrossRef]
54. Zorębski, E. Internal pressure as function of pressure for alkanols. *Mol. Quant. Acoust.* **2007**, *28*, 319–326.
55. Dzida, M. Study of the effects of temperature and pressure on the thermodynamic and acoustic properties of 2-methyl-1-butanol at temperatures from (293 to 318) K and pressures up to 100 Mpa. *Int. J. Thermophys.* **2010**, *31*, 55–69. [CrossRef]
56. Zorębski, E.; Musiał, M.; Dzida, M. Relation between temperature-pressure dependence of internal pressure and intermolecular interactions in ionic liquids—Comparison with molecular liquids. *J. Chem. Thermodyn.* **2019**, *131*, 347–359. [CrossRef]